IL NUOVO CIMENTO Vol. 34 C, N. 2 Marzo-Aprile 2011
DOI 10.1393/ncc/i2011-10831-0

Colloquia: WISH2010

Charmonium production with the ALICE experiment at LHC

F. Fionda for the ALICE Collaboration
Dipartimento Interateneo di Fisica "M. Merlin" and INFN, Sezione di Bari - Bari, Italy

(ricevuto il 17 Gennaio 2011; approvato il 24 Gennaio 2011; pubblicato online il 16 Marzo 2011)

Summary. — According to theoretical predictions charmonium production in nucleus-nucleus collisions at LHC energy could be a nice example of interplay between "hard" and "soft" aspects of QCD interactions. In fact the c and $\bar{c}$ quarks are indubitably produced in "hard" partonic scattering, but a new "soft" mechanism at LHC could become relevant for the charmonium production in Pb-Pb collisions: "coalescence" may lead free c and $\bar{c}$ quarks in the QGP to recombine into charmonium mesons. The ALICE detector at LHC will measure charmonium production both at central and forward rapidity using two different decay channels, and reaching in both cases down to $p_{\mathrm{T}} = 0$. The first results in proton-proton collisions for the charmonium measurements will be discussed in this contribution.

PACS 14.40.Pq – Heavy quarkonia.
PACS 25.75.Nq – Quark deconfinement, quark-gluon plasma production, and phase transitions.

1. – Quarkonium production in ultra-relativistic collisions

Quarkonium production measurement in proton-proton collisions is of great importance, not only as a reference for heavy ion, but also in itself since the production mechanism for quarkonia is not completely understood yet. It also provides a window for the study of the gluon structure of nucleons and its modification in nuclei. Concerning the high-energy collisions of heavy nuclei it provides a very important means of studying the hot-dense matter, and it is a critical probe to look for deconfinement.

1˙1. *Proton-proton collisions*. – There are several models available to describe quarkonium production in hard partonic scattering but none succeeded to predict simultaneously measured cross-sections and polarization.

The first model, proposed shortly after the discovery of the J/ψ [1, 2], was the color-singlet-model (CSM) [3]. In this picture charmonia and bottomonia mesons are presumed to exclusively originate from short-distance processes that create heavy-quark pairs in a color-singlet configuration. In this picture $q\bar{q}$ pairs are created by parton collisions with negligible relative momentum and those can bind together into quarkonia states,

only if the pair is initially created colorless and with angular-momentum configuration as in the quarkonia state (for example 1^3S_1 for J/ψ). The CSM has been considered until 1995, when the CDF experiment at the Tevatron [4] showed that it under-predicts cross-sections for charmonium production by more than an order of magnitude. More recent revisitations of CSM (*i.e.* CSM+s-channel cut) [5] compared with measurements done at RHIC by the PHENIX experiment show that CSM works properly to reproduce cross-sections at forward rapidity, but fails to predict the J/ψ polarization especially at forward rapidity [6].

Although the heavy-quark production implies perturbative processes, there are also non-perturbative effects associated with the dynamics of the quarkonium bound state that invalidate the direct application of perturbation theory. In order to apply the perturbative methods, it is needed to separate first short-distance/high-momentum effects from the long-distance/low-momentum ones, and this process is known as "factorization". One convenient way to consider this separation is by the use of an effective field theory, based on nonrelativistic QCD (NRQCD) [7]. The NRQCD Lagrangian can be considered as a sum of "long-distance" operators and each one is multiplied by a "short-distance" coefficient, which encodes the ultraviolet physics. This effective field theory, which sometimes is called color-octet-model (COM), generalizes and improves the CSM in several regards. It allows for short-distance processes to create heavy quark-antiquark pairs in color-octet configurations which can hadronize over much longer length scales into colorless final state quarkonia. Calculations which include this color-octet mechanism can successfully describe Tevatron measurements of charmonium cross-sections, but fail completely to predict polarization [8].

Finally the color evaporation model (CEM) is based purely on "phenomenological" grounds [9]. According to this model, the cross-section for the production of a quarkonium state H is the fraction F_H (dependent on the state H) of the cross-section for producing $q\bar{q}$ pairs with invariant mass below $M\bar{M}$ threshold, where M is the lowest mass meson containing the heavy quark q. There are no constraint on the color or spin of the final state, there is only an upper limit on the $q\bar{q}$ pair mass. The color-evaporation model has the advantage to be relatively easy to use with respect to the others, but its predictive power is limited only for inclusive productions, and it does not predict polarization.

1˙2. *Nucleus-nucleus collisions.* – In relativistic heavy-ion collision, the strongly interacting matter is predicted to undergo a phase transition into a plasma of deconfined quarks and gluons (QGP) and quarkonia probe different aspects of this medium. In the seminal prediction by Matsui and Satz, the so-called "J/ψ anomalous suppression", the charmonia states could melt in deconfined medium [10]. Above the critical temperature quarks and gluons become deconfined color charges, and this quark-gluon plasma leads to a color-screening which limits the range of strong interaction. The color screening radius r_D, which determines this range, is inversely proportional to the density of charges, so that it decreases with increasing temperature. Each quarkonium state has a proper dissociation temperature, which is called "Debye temperature": the quarkonium would melt only if this dissociation temperature is reached in the QGP.

It is possible to suppose the existence of different quarkonia production mechanisms at very high energies: the hard partonic scattering, as in proton-proton, whereby charmonia are produced at the early stage of collision, as well as a "soft" production mechanism. This "soft" hypothesis is corroborated by the observation of similar J/ψ suppression at RHIC and SPS [11, 12], although the energy density is higher at RHIC and therefore suppression was expected to be stronger. Moreover, the suppression is stronger (by

$\sim 40\%$) at forward rapidity [11, 12] compared to mid-rapidity while the suppression scenario, suggested by the Debye screening, would predict the opposite trend (the latter observation can also be explained by cold nuclear matter (CNM) effects [13] which are different at mid-rapidity and forward rapidity). This "soft" process consists in a "regeneration" for charmonia: deconfined $q\bar{q}$ pairs can recombine together to form quarkonia by "coalescence" [14]. Other models describe the same mechanism, *e.g.*, the "statistical hadronization", where quarkonium production takes place at the phase boundary with statistical weights [15].

Whereas the relative importance of this regeneration mechanism at RHIC energies is still under debate ([16] *vs.* [17]), there is a general agreement to believe that LHC is the domain where regeneration for charmonia becomes relevant.

Moreover, thanks to higher center-of-mass energy at LHC, it will be possible to measure the production of bottomonia states which are also sensitive to the production mechanism: in particular the bottomonia state $\Upsilon(1S)$ is expected to be melt only at LHC due to its high Debye temperature. In addition, the "regeneration" for bottomonia is an interesting question to be addressed ad LHC. The $\Upsilon(2S)$ is expected to behave as the J/ψ ($T^D_{\Upsilon(2S)} \sim T^D_{J/\psi}$) and assuming that at LHC bottomonia are not affected by regeneration, $\Upsilon(2S)$ measurements would be fundamental for understanding J/ψ suppression *versus* regeneration.

2. – The ALICE detector at LHC

ALICE (A Large Ion Collider Experiment), which is designed for heavy ion physics, has also an important program with proton-proton collisions. It is divided into a barrel, that covers the $|\eta| < 0.9$ region with a magnetic field of 0.5 T, and a forward muon arm that covers the region $-4 < \eta < -2.5$. A detailed description of the ALICE set up can be found in [18]. With its apparatus ALICE can perform quarkonia measurements in both central region, in the dielectron channel ($J/\psi \to e^+e^-$) and forward rapidity region in the dimuon channel ($J/\psi \to \mu^+\mu^-$), reaching in both cases $p_T = 0$.

2˙1. *Central barrel.* – The main tracking detectors in the barrel are the Inner Tracking System (ITS) and the Time Projection Chamber (TPC). The ITS, which is the vertex detector for open heavy flavour physics, is made up of 6 layers of silicon detectors, realized in different technologies: from inner to outer there are two layers of Silicon Pixel (SPD), Silcon Strip (SSD) and Silicon Drift (SDD) detectors. Thanks to the ITS, the spatial resolution will allow to measure the fraction of J/ψ "displaced" from primary vertex, *i.e.* coming from beauty hadrons decay.

The TPC, designed to reconstruct more than 15000 primary tracks in central Pb-Pb collisions, is the main tracking device of ALICE and gives up to 160 spatial points. It has an excellent Particle IDentification for particles with intermediate momenta, based on the measurement of their specific energy loss.

Besides the TPC, the PID in central barrel (in particular for electrons) is realized by adding the information of the Time Of Flight detector (TOF), which helps to reject protons and pions for momenta below $\sim 1.5\,\mathrm{GeV}/c$, and the Transition Radiation Detector (TRD), which is dedicated to the electron-pion discrimination([1]).

([1]) The TRD has not been used in the present preliminary analysis.

2˙2. *Muon spectrometer*. – The Forward Muon Spectrometer of the ALICE experiment is designed for the study of quarkonium resonances and open heavy flavour particles. It is composed by several hadron absorbers: a front absorber made by carbon, concrete and steel especially optimized to limit scattering and energy loss in the muon path; a muon filter which consists of an iron wall and allows to reduce the low-energy particle background in the trigger chambers; a beam shield around the beam pipe made by lead and tungsten to reduce low-energy background due to secondary interactions along the pipe. The reconstruction of tracks is performed by 5 stations of high granularity tracking chambers, which are multiwire proportional chambers with two-cathode pad-segmented read-out. The tracking station 3 is placed inside a dipole magnet with a total field integral $\mathrm{B} \cdot l = 3\,\mathrm{Tm}$. The spatial resolution measured in beam test is of the order of $70\,\mu\mathrm{m}$ in the bending plane. Finally, two stations of trigger chambers equipped with two planes of Resistive Plate Chambers each, are located downstream of the tracking system (after the iron wall). Those are useful to reduce the background from the remaining hadrons and secondary muons produced in the absorber.

3. – Data taking and first results

ALICE has collected the first proton-proton data in November 2009 at $\sqrt{s} = 900\,\mathrm{GeV}$. The center-of-mass energy value was increased to $\sqrt{s} = 2.36\,\mathrm{TeV}$ in December 2009. From March 2010 LHC has started its program at $\sqrt{s} = 7\,\mathrm{TeV}$. The samples of events used in this analysis refer to the latter period. They are different in central barrel and in the

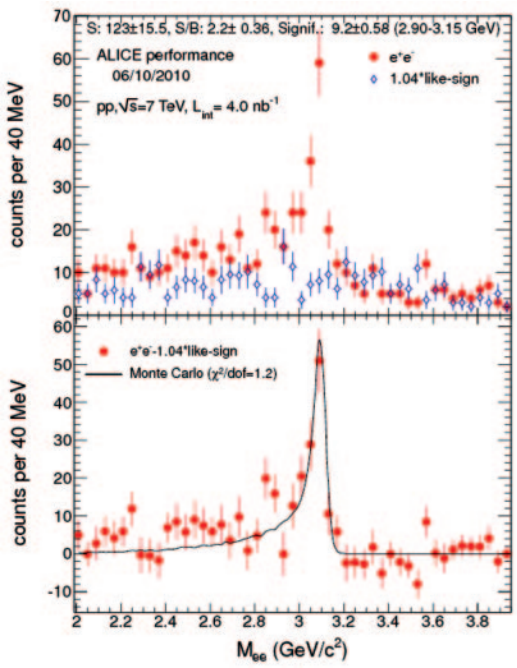

Fig. 1. – (Color online) Top panel: invariant mass of unlike-sign selected tracks (red circles) and the same for like-sign pairs (blue circles). Bottom panel: invariant mass distribution of unlike-sign pairs after subtracting the like-sign distribution. The black line is the Monte Carlo shape.

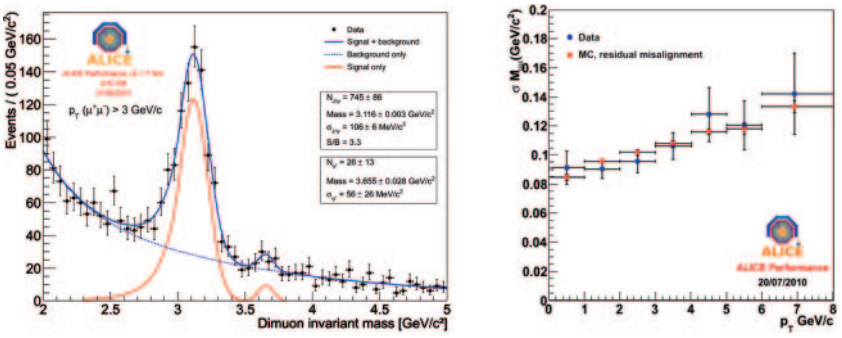

Fig. 2. – (Color online) Left: invariant mass distributions for J/ψ and ψ' candidates, requiring that at least one of the two daughter tracks matches a muon trigger track and the transverse momentum of candidates is greater than 3 GeV. The fit is performed by a Cristal Ball [19] for the J/ψ mass peak, a Gaussian for the ψ' and two exponentials for the background. Right: measured resolution (blue points) on J/ψ invariant mass as a function of p_{T} compared with Monte Carlo simulations (red points). The residual misalignment is included in the simulations.

muon spectrometer because they have been collected with different detector and trigger configurations. For central barrel, events were selected by a "minimum-bias" trigger and the relevant detectors are the two most inner layers of ITS (SPD) and the scintillator counters VZERO [18]: the requirement was at least one hit in SPD combined in logical or with one signal in VZERO counters. The number of "minimum-bias" events collected until September 1st is around $69.4 \cdot 10^7$.

In the central barrel the J/ψ is identified in the dielectron channel and the analysis strategy is based on the identification of the electrons. Figure 1 (top panel) shows the the invariant mass distribution of unlike (red circles) and like (blue circles) sign pairs. The single track selection was based on several track quality criteria, such as the number of clusters found in the TPC (more than 90), the requirement of at least one point in the first layer of the SPD and the transverse momentum larger than 1 GeV. For the PID, only the TPC has been used so far: in particular selected tracks are within the 3σ band around the $\mathrm{d}E/\mathrm{d}x$ electron line of the Bethe-Bloch parametrization, and outside the 3σ pion and proton bands, in order to reduce pion and proton contamination. The result obtained subtracting the two distributions compared with Monte Carlo signal (black line) is shown in the bottom panel.

The muon spectrometer has collected data using the "minimum-bias" trigger in parallel with the "muon trigger". The latter selects events where at least one track tagged as a muon passes through the muon spectrometer. Besides the "minimum-bias" trigger events the analysis in the dimuon channel includes also the sample of "muon trigger" events at 7 TeV, which is around $47 \cdot 10^6$ (collected until September 1st). A crucial aspect for the muon spectrometer is the alignment of the tracking chambers. The achieved mass resolution is close to the nominal value, which is 70 MeV/c^2, as an outcome of alignment with null magnetic field. The performance plot obtained is shown in fig. 2 (left panel). The requirements are that at least one of the two daughter tracks matches a muon trigger track and the transverse momentum of candidates is greater than 3 GeV. The fits are made by a Cristal Ball function for the signal and two exponentials for the background (plus a Gaussian for the ψ' peak). The statistics collected by the muon spectrometer, which benefits from the available muon trigger, is enough to allow the measurement of

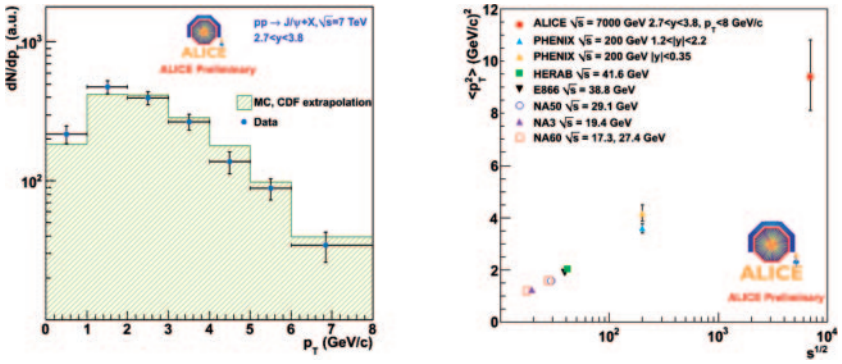

Fig. 3. – (Color online) Left: transverse momentum distribution (blue points) corrected for acceptance and efficiency. For comparison Monte Carlo distribution obtained from CDF extrapolation is shown. Right: $\langle p_{\mathrm{T}}^2 \rangle$ as a function of the center-of-mass energy for different experiments; the red point is the ALICE preliminary measurement.

the transverse momentum dependence of both signal and resolution extrapolated from J/ψ invariant mass distributions. Figure 2 (right panel) shows the measured resolution (blue points) on J/ψ invariant mass as a function of p_{T} compared with Monte Carlo simulations. The residual misalignment is included in the simulations.

The application of the acceptance and efficiency corrections to the number of reconstructed signal candidates leads to the corrected yield of J/ψ as a function of p_{T}, which can be fitted in order to obtain the mean transverse momentum $\langle p_{\mathrm{T}} \rangle$, as well as the mean-square transverse momentum $\langle p_{\mathrm{T}}^2 \rangle$. The transverse momentum distribution (blue points) after the application of the acceptance and efficiency corrections compared with Monte Carlo distribution obtained from CDF extrapolation is shown in fig. 3 (left panel). Figure 3 (right panel) shows the $\langle p_{\mathrm{T}}^2 \rangle$ as a function of $\sqrt{s}$: the points are from different experiments of SPS and RHIC, the red one is the ALICE preliminary measurement. This is found to be larger by a factor 2–2.5 with respect to the estimation performed by RHIC at $\sqrt{s} = 200\,\mathrm{GeV}$.

4. – Conclusion

The ALICE experiment is currently taking data with very good detector performance, and will soon deliver a measurement of J/ψ production in p-p collisions at $\sqrt{s} = 7\,\mathrm{TeV}$ at central and forward rapidity, reaching in both cases $p_{\mathrm{T}} = 0$.

A rich measurement program is foreseen for the first Pb-Pb run at LHC. The very first data in Pb-Pb collisions has resulted in interesting first glimpses into the QCD matter created at LHC [20, 21].

REFERENCES

[1] Aubert J. J. *et al.*, *Phys. Rev. Lett.*, **33** (1974) 1404.
[2] Augustin J. E. *et al.*, *Phys. Rev. Lett.*, **33** (1974) 1406.
[3] Schuler G. A., hep-ph/9403387 (1994).
[4] Abe F. *et al.*, *Phys. Rev. Lett.*, **75** (1995) 4358.
[5] Campbell J., Maltoni F. and Tramontano F., *Phys. Rev. Lett.*, **98** (2007) 252002.

[6] Linden Levy L. A., *Nucl. Phys. A*, **830** (2009) 353c.
[7] Bodwin G. T., Braaten E. and Lepage G. P., *Phys. Rev. D*, **51** (1995) 1125.
[8] CDF Collaboration, *Phys. Rev. Lett.*, **99** (2007) 132001.
[9] Fritzsch H., *Phys. Lett. B*, **67** (1977) 217.
[10] Matsui T. and Satz H., *Phys. Lett. B*, **178** (1986) 416.
[11] Alessandro B. *et al.*, *Eur. Phys. J. C*, **39** (2005) 335.
[12] Adare A. *et al.*, *Phys. Rev. Lett.*, **98** (2007) 232201.
[13] Lansberg J. P. *et al.*, *AIP Conf. Proc.*, **1038** (2008), pp. 15-44.
[14] Thews R. L., Schroedter M. and Rafelski J., *Phys. Rev. C*, **63** (2001) 054905.
[15] Braun-Munziger P. and Stachel J., *Phys. Lett. B*, **490** (2000) 196.
[16] Andronic A., Braun-Munzinger P., Redlich K. and Stachel J., *Phys. Lett. B*, **652** (2007) 259.
[17] Rapp R. and Grandchamp L., *Nucl. Phys. A*, **709** (2002) 415.
[18] Aamodt K. *et al.* (ALICE Collaboration), *J. Instrum.*, **3** (2008) S08002.
[19] Gaiser J. E., *Phys. Rev. D*, **34** (1986) 711.
[20] ALICE Collaboration, *Phys. Rev. Lett.*, **105** (2010) 252301.
[21] ALICE Collaboration, *Phys. Rev. Lett.*, **105** (2010) 252302.